Impact of Siberian coastal polynyas on shelf-derived Arctic Ocean halocline waters

Dorothea Bauch,[1,2] Jens A. Hölemann,[3] Igor A. Dmitrenko,[1] Markus A. Janout,[3] Anna Nikulina,[2] Sergey A. Kirillov,[4] Thomas Krumpen,[3] Heidemarie Kassens,[1] and Leo Timokhov[4]

Received 16 May 2011; revised 4 January 2012; accepted 16 February 2012; published 5 April 2012.

[1] Hydrographic and stable oxygen isotope ($H_2^{18}O/H_2^{16}O$) sampling was carried out within the West New Siberian (WNS) coastal polynyas in the southern Laptev Sea in late winters 2008 and 2009. The impact of sea ice formation on the water column was quantified by a salinity/$\delta^{18}O$ mass balance. Several stations had vertically homogeneous physical properties in April/May 2008 and featured polynya-formed local bottom water with elevated signals of brine released during sea ice formation and elevated fractions of river water. The polynya-formed bottom water was fresher than surrounding bottom waters. At other stations, salinity/$\delta^{18}O$ correlation showed well-defined mixing lines for bottom and surface layers. In March–April 2009, surface waters were strongly influenced by Lena River water, and local polynya activity with elevated brine signals reached to intermediate depth but did not penetrate the bottom layer in the highly stratified water column. Inventory values of sea ice formation were comparable in both years, but freshwater distributions from the preceding summers were different. Therefore, the observed difference in the impact of polynya activity on the water column is not primarily controlled by the amount of sea ice formed during winter but by preconditioning from the preceding summer. Only in years when the river plume is mostly absent in the polynya region is stratification weak and allows winter sea ice formation to reach the bottom layer. Thus summer stratification controls the influence of local polynya water on the shelf's bottom hydrography and, as bottom water is exported, impacts on the source water of shelf-derived halocline waters.

Citation: Bauch, D., J. A. Hölemann, I. A. Dmitrenko, M. A. Janout, A. Nikulina, S. A. Kirillov, T. Krumpen, H. Kassens, and L. Timokhov (2012), Impact of Siberian coastal polynyas on shelf-derived Arctic Ocean halocline waters, *J. Geophys. Res.*, *117*, C00G12, doi:10.1029/2011JC007282.

1. Introduction

[2] The dramatic reduction in summer Arctic sea ice extent and thickness in recent years [e.g., *Comiso et al.*, 2008; *Kwok and Rothrock*, 2009; *Kwok et al.*, 2009] has been accompanied by substantial warming of the Arctic Ocean Atlantic layer [*Schauer et al.*, 2004; *Polyakov et al.*, 2007; *Dmitrenko et al.*, 2008a]. An important feature of the Arctic Ocean is the cold and fresh halocline insulating the sea ice cover from the underlying warm Atlantic layer [*Coachman and Barnes*, 1963; *Aagaard et al.*, 1985; *Steele and Boyd*, 1998]. The Siberian shelves supply freshwater into the Arctic Ocean halocline and are main production areas for sea ice [*Aagaard et al.*, 1981]. As a result of sea ice formation brine-enriched bottom waters are produced on the shelf and exported to the Arctic Ocean halocline [*Bauch et al.*, 2009a], as well as to the Arctic Ocean bottom and deep waters [*Bauch et al.*, 1995]. Thus, it is important to understand the shelf processes and the likely feedback between sea ice processes and the ongoing climate change with its related strongly reduced summer sea ice cover.

[3] On the shallow Siberian shelves persistent offshore winds create areas of open water in the winter sea ice cover at the border between the land-fast ice and the pack ice at about 30 m water depth [*Bareiss and Görgen*, 2005]. This recurring phenomenon is known as the Great Siberian Polynya and may be up to 200 km wide [*Zakharov*, 1966, 1997] (Figure 1). Due to large vertical salinity gradients in the Laptev Sea, which are enhanced by summer discharge from the Lena River, stratification is generally preserved throughout the winter [*Bauch et al.*, 2009b; *Dmitrenko et al.*, 2005a, 2010a]. Thus the long-term mean probability for convective mixing down to the seafloor is only about 20% to 70% for the eastern and western Laptev Sea, respectively [*Dmitrenko et al.*, 2005a; *Krumpen et al.*, 2011b]. Accordingly, the impact of winter sea ice formation may vary significantly on inter-annual time scales and a change in the vertical distribution of this impact was observed in the

[1]GEOMAR Helmholtz Centre for Ocean Research Kiel, Kiel, Germany.
[2]Academy Mainz, c/o GEOMAR, Kiel, Germany.
[3]Alfred Wegener Institute for Polar and Marine Research, Bremerhaven, Germany.
[4]Arctic and Antarctic Research Institute, St. Petersburg, Russia.

Copyright 2012 by the American Geophysical Union.
0148-0227/12/2011JC007282

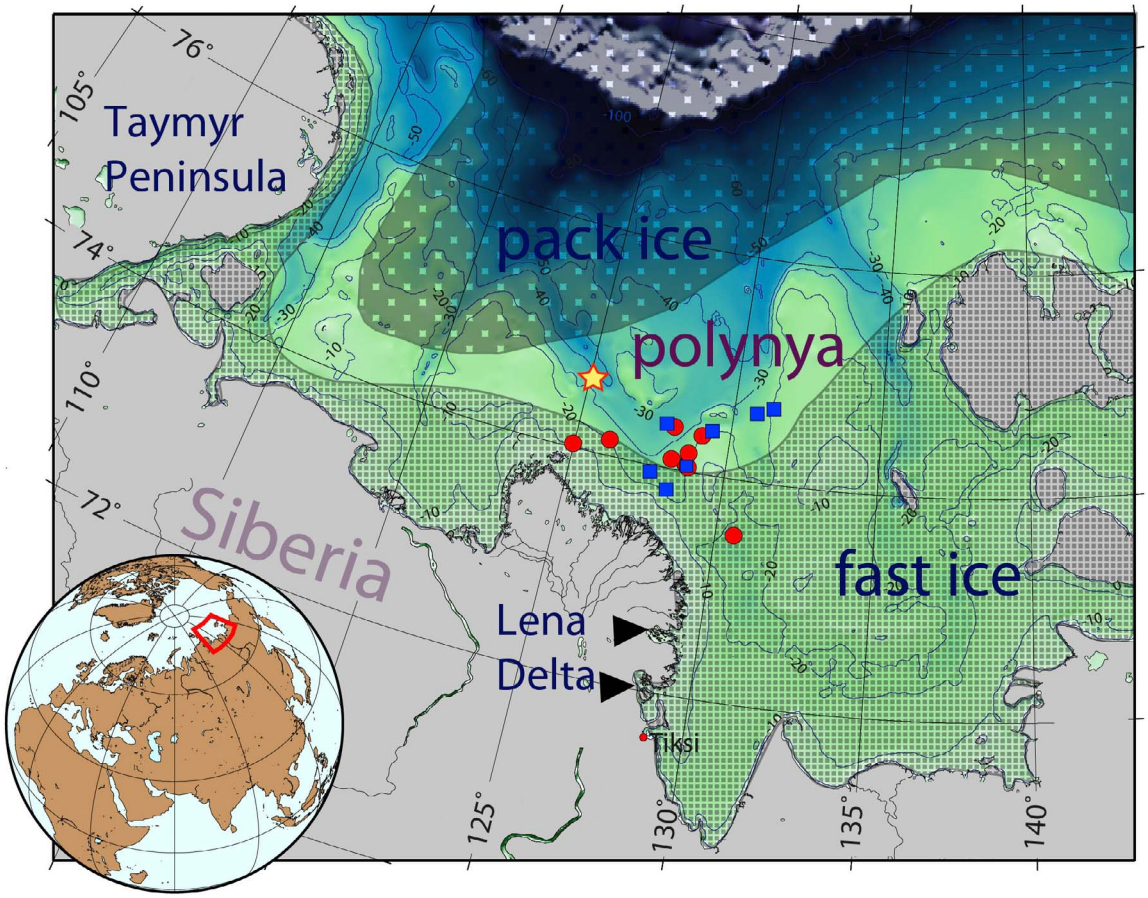

Figure 1. Geographical map of the Laptev Sea (region outlined on the globe) and stations occupied during winter expeditions TI08 (squares) and TI09 (dots). Also indicated are the position of mooring Khatanga (74°42.9′N, 125°17.4′E; star) [*Hölemann et al.*, 2011], and the average position of the recurring coastal polynya [*Zakharov*, 1997] between the area of the fast ice and pack ice. The triangles indicate the main outlets of the Lena River.

eastern Laptev Sea in summer 2007 [*Bauch et al.*, 2010]. The factors responsible for this qualitative difference are not understood and it is an open question, whether they are related to climate change and reduced summer sea ice cover.

[4] This study examines the role of the Laptev Sea polynya in modifying the Laptev Sea shelf hydrography based on late winter field observations in April–May 2008 and March–April 2009. Our study is based on observations of the oxygen isotope composition ($\delta^{18}O$) of the water in conjunction with hydrological data that allows quantifying the effect of sea ice melting or formation on the water column. We aim to assess under which conditions the Laptev Sea coastal polynya influences the surface waters only and under which conditions it is able to influence the bottom layer of the Laptev Sea and thereby the Arctic Ocean halocline.

2. Sample Collection and Measurement

[5] As a part of the Russian-German project "Laptev Sea System," a winter field program was conducted in the Laptev Sea coastal polynya region. Between 11 April and 4 May 2008 (TI08) and between 24 March and 23 April 2009 (TI09) hydrographic stations were occupied by helicopter at distances 10 to 800 m inland from the fast ice edge of the West New Siberian (WNS) coastal polynya (Figure 1). Typical water depths were 20 to 35 m. Routine CTD observations were carried out from the 40–170 cm thick ice cover, with the instrument lowered through a 22 cm diameter hole drilled through the ice. Water samples were collected with Niskin bottles directly after CTD casts were completed. Individual temperature and conductivity measurements are accurate to $\pm$ 0.005°C and $\pm$ 0.0005 S/m, respectively, for the SBE-19+, and $\pm$ 0.002°C and $\pm$ 0.0003 S/m for the SBE-37s used during TI08 and TI09, respectively. Detailed hydrographic conditions and results of moorings deployed at a subset of the stations are presented elsewhere [*Dmitrenko et al.*, 2010a, 2010b]. The evolution of the WNS polynya during 2008 and 2009 was continuously monitored with Environmental Satellite (ENVISAT) Advanced Synthetic Aperture Radar (SAR) images. For further details see *Dmitrenko et al.* [2010b] and *Krumpen et al.* [2011a, 2011b].

[6] Oxygen isotopes of seawater from TI08 and TI09 were analyzed at the Stable Isotope Laboratory of COAS at Oregon State University (Corvallis, USA) applying the CO_2- water isotope equilibration technique and analyzed by dual inlet mass spectrometry on a DeltaPlus XL. The overall measurement precision for all $\delta^{18}O$ analysis is $\pm$ 0.04‰. The

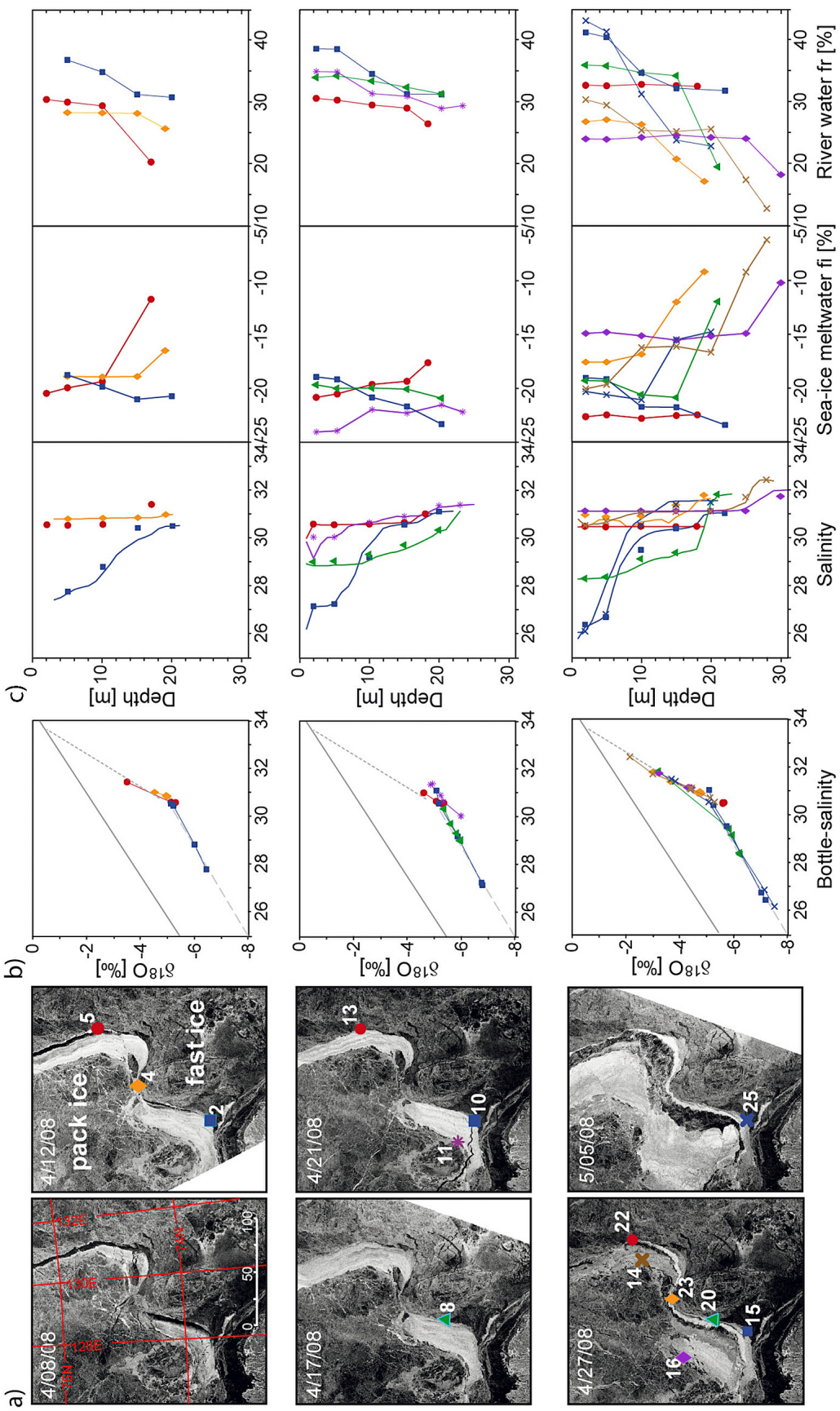

Figure 2. Station data from TI08 in the southeastern Laptev Sea from 11–14 April, 16–21 April, and 21 April to 4 May 2008. Station data are shown with corresponding symbols at each position in (a) ENVISAT synthetic aperture radar (SAR) images and for (b) $\delta^{18}O$ versus salinity (bottle data) and (c) depth profiles of CTD (1 m averages) and bottle salinity versus depth as well as fractions of sea ice meltwater f_i and river water f_r. Negative f_i values represent the amount of water removed during sea ice formation and are proportional to brine released during sea ice formation; for further explanation, see text. Dates of ENVISAT SAR images are indicated. Please note that the polynya is situated between the pack ice and fast ice area. and open water or thin ice appears either black or white, respectively.

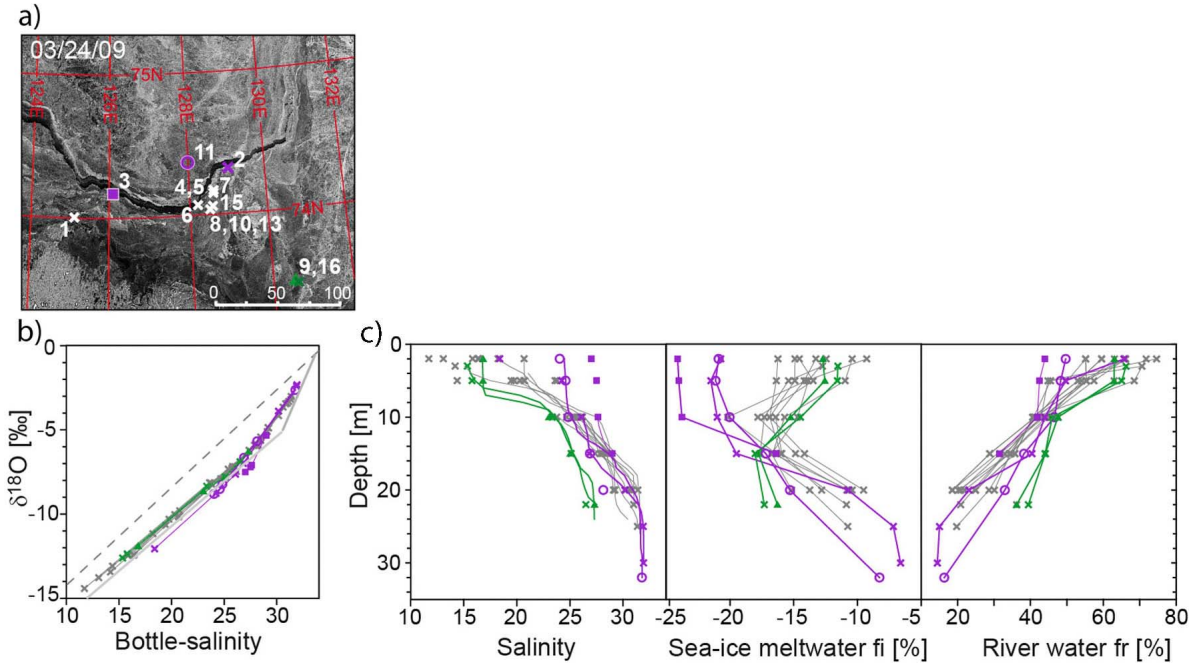

Figure 3. Station data from TI09 in the southeastern Laptev Sea from 24 March to 23 April 2009. Station positions are shown in (a) ENVISAT SAR image from 24 March, and station data are shown in corresponding symbols for (b) $\delta^{18}O$ versus salinity (bottle data) and (c) depth profiles of CTD (1 m averages) and bottle salinity as well as fractions of sea ice meltwater f_i and river water f_r.

$^{18}O/^{16}O$ ratios are calibrated with VSMOW and reported in the usual δ-notation [*Craig*, 1961].

[7] Salinity data is reported on the psu scale. For a quantitative interpretation of our data an exact match of salinity and $\delta^{18}O$ values is essential. Therefore, in addition to CTD measurements, bottle salinity was determined directly within the water samples taken for $\delta^{18}O$ analysis using an AutoSal 8400A salinometer (Fa. Guildline) with a precision

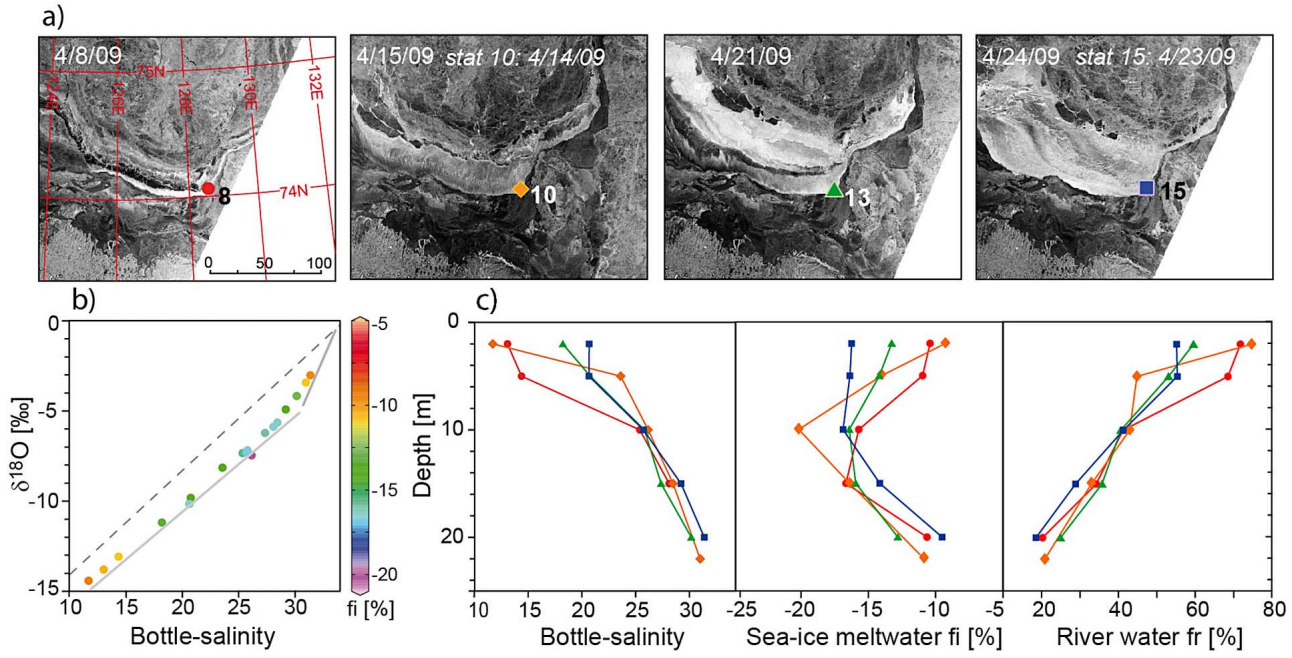

Figure 4. Station data from TI09 at ~131.25°E and ~74.67°N for stations 8, 10, 13, and 15 sampled on 8, 14, 21, and 23 April 2009, respectively: (b) $\delta^{18}O$ versus salinity (bottle data) with colored dots for sea ice meltwater fractions f_i and (c) depth profiles of salinity and fractions of sea ice meltwater f_i and river water f_r. (a) Station positions are shown in ENVISAT SAR images with corresponding symbols.

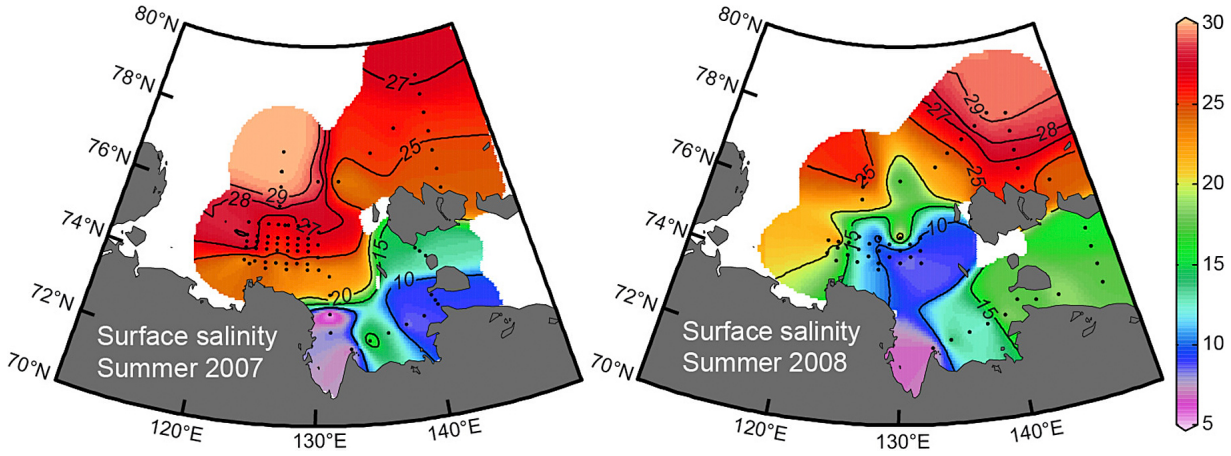

Figure 5. Surface salinities of summer expeditions in September 2007 and in September 2008. Stations positions are indicated by small black dots.

of ±0.003 and an accuracy greater than ±0.005. While the CTD salinity data has a sufficiently high precision, CTD and bottle data on a shallow shelf are not exactly matched when aligned by depth (see Figure 2c and Figure 3c) due to differences in spatial and temporal alignment of the instruments during successive sampling (for further details, see *Bauch et al.* [2010]). CTD-derived and bottle salinities for station TI08–5 show an offset due to frazil ice in the conductivity sensor and conductivity measurements were omitted for this station.

3. Hydrography of the Laptev Sea and Hydrographic Results

[8] The vast Siberian shelf regions cover more than one third of the total Arctic Ocean area and receive fresh water from several large rivers, primarily the Ob and Yenisey rivers in the Kara Sea and the Lena River in the Laptev Sea (see Figure 1). The Lena River is one of the largest Siberian rivers and releases runoff onto the Laptev Sea shelf predominantly during summer [e.g., *Létolle et al.*, 1993]. Our study area is directly north of the Lena River delta in the southeastern Laptev Sea (Figure 1) and receives on average 435 km^3 of river water in summer (June–September), while during winter (November–April) the discharge is only about ~38 km^3 (Arctic-RIMS data, http://rims.unh.edu). During winter the Laptev Sea is ice covered and polynyas and flaw leads are opened repeatedly by offshore winds and produce large amounts of sea ice accordingly [*Willmes et al.*, 2011; *Bareiss and Görgen*, 2005; *Zakharov*, 1966]. Estimated ice volume produced in the southeastern Laptev Sea study area e.g., in winter 2007/8 was ~81 km^3 [*Krumpen et al.*, 2011b]. The fast ice in the southern Laptev Sea breaks up in June and July at the time of the main river discharge. Sea ice cover retreats over the entire Laptev Sea mainly during July and August and recurs in October.

[9] During both sampling periods in late winters 2008 (Figure 2) and 2009 (Figures 3 and 4) the West New Siberian (WNS) coastal polynya was within its typical range of positions (Figure 1). Hydrographic conditions in the study region were similar in bottom salinities but surface salinities were considerably lower in April 2009. Salinities ranged from ~26 to 32.5 in April 2008 (Figure 2b) and from ~12 to 32 in April 2009 (Figure 3b). These differences in stratification were also seen in the study area in the preceding summers (Figure 5) [see also *Dmitrenko et al.*, 2010a].

4. Stable Isotope Derived Signal of Sea Ice Formation

[10] The distributions of salinity and δ^{18}O in the water column are quite similar as they are, to first order, linearly correlated (Figure 6). River water in the Arctic is highly depleted in its stable oxygen isotope composition (δ^{18}O) and an admixture of river water can be identified by its reduced δ^{18}O signal and low salinity relative to marine waters. Sea ice melting and formation on the other hand can be separated from any mixture between marine and river water since it strongly influences salinity whereas the δ^{18}O signal remains nearly unaltered.

4.1. Calculation of River Water and Sea Ice Meltwater Fractions

[11] The river water and sea ice meltwater contributions can be quantified by applying a mass balance calculation [e.g., *Östlund and Hut*, 1984; *Schlosser et al.*, 1994; *Bauch et al.*, 1995]. In this calculation it is assumed that each sample is a mixture between marine water (f_{mar}), river-runoff (f_r) and sea ice meltwater (f_i). The balance is governed by the following equations:

$$f_{mar} + f_r + f_i = 1,$$
$$f_{mar} * S_{mar} + f_r * S_r + f_i * S_i = S_{meas},$$
$$f_{mar} * O_{mar} + f_r * O_r + f_i * O_i = O_{meas},$$

where f_{mar}, f_r and f_i are the fractions of marine water, river-runoff and sea ice meltwater in a water parcel, and S_{mar}, S_r, S_i, O_{mar}, O_r and O_i are the corresponding salinities and δ^{18}O values (Table 1). S_{meas} and O_{meas} are the measured salinity and δ^{18}O of the water samples.

[12] For the marine water end-member we use the values of the Atlantic inflow in the Eurasian Basin with 34.92 in salinity and 0.3‰ in δ^{18}O [*Bauch et al.*, 1995]. Average δ^{18}O of Arctic rivers is about −20‰ [*Bauch et al.*, 1995; *Frank*,

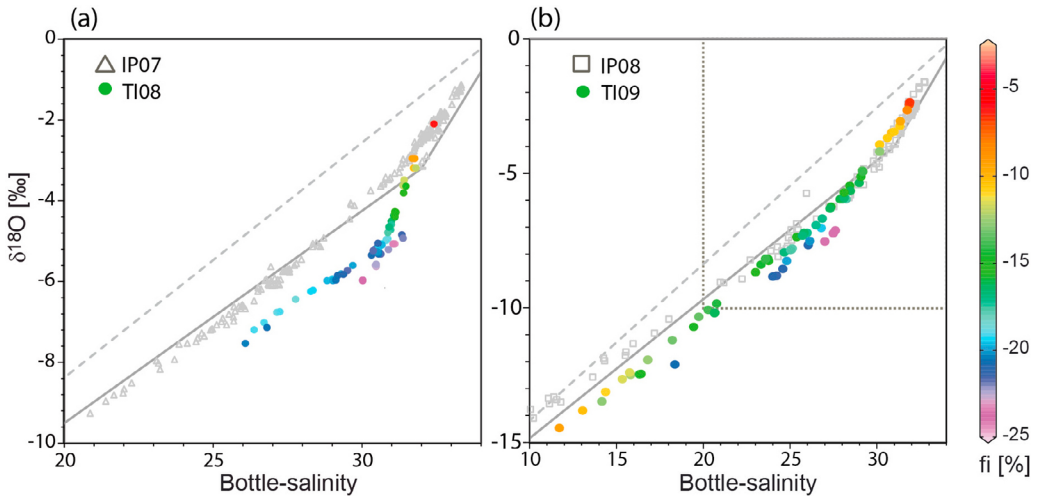

Figure 6. The $\delta^{18}O$ versus salinity for winter expeditions (a) TI08 and (b) TI09 (colored dots) together with preceding summer data from the study area in summer 2007 (gray triangles) and 2008 (gray squares), respectively. The coloring of dots represents the sea ice meltwater fraction f_i for each sample. The mixing line between marine and river end-member values is indicates for orientation (gray stippled) as well as summer data mixing lines (gray). Note different scales for $\delta^{18}O$ and salinity for TI08 and TI09 (smaller range of Figure 6a for TI08 is indicated by gray dotted frame in Figure 6b for TI09).

1996] and taken as river water end-member. Within uncertainties this choice matches the average Lena River $\delta^{18}O$ value of −19.5‰ derived from linear interpolation to zero salinity [*Bauch et al.*, 2010] and also the flow-weighted average of −20.5‰ based on all-season measurements [*Cooper et al.*, 2008]. For sea ice meltwater the $\delta^{18}O$ value of surface water at each station together with a fractionation of +2.6‰ [*Melling and Moore*, 1995] is taken as an end-member and a salinity of 4 as measured for multiyear ice [*Pfirman et al.*, 2004]. Negative sea ice meltwater fractions f_i reflect the amount of water removed by sea ice formation and are proportional to the subsequent addition of brines to the remaining water column. In this manuscript negative sea ice meltwater fractions are also referred to as brine signal due to sea ice formation or just brine signal. All fractions are net values reconstructed from the $\delta^{18}O$ and salinity signature of each sample and reflect the time integrated effects on the sample volume.

[13] The analytical errors arise from $\delta^{18}O$ and salinity measurements and add up to approximately ± 0.3% for each of the fractions but the additional systematic error depends on the exact choice of end-member values. Variations in the choice of end-member values within the estimated uncertainties (Table 1) shifts absolute values, by up to ∼1% in both fractions [see also *Bauch et al.*, 2011a] but relative results are always conserved even when extreme variations in end-member values are tested.

4.2. Results of $\delta^{18}O$/Salinity Mass Balance Analysis

[14] Calculated fractions of river water generally decrease with depth for TI08 (Figure 2c) and TI09 (Figure 3c). River water fractions are 24–43% and 44–75% in the surface layer for TI08 and TI09, respectively. In the bottom layer river water fractions are 13–32% for TI08 and 14–39% for TI09. Although river water fractions in the surface layer tend to be higher toward the southeast in Laptev Sea summer data [*Bauch et al.*, 2009a, 2010] there are no clear geographical gradients within the comparatively small study area in winter.

[15] Fractions of sea ice meltwater are negative for all samples taken during winter expeditions TI08 and TI09. Generally the influence of brines released by sea ice formation (negative f_i) decreases with depth during TI08 and TI09 (Figures 2 and 3). Surface layer sea ice meltwater fractions f_i were −15 to −24% and −9 to −24% for TI08 and TI09, respectively. In the bottom layer sea ice meltwater fractions f_i were −6 to −23% and −7 to −17% for TI08 and TI09, respectively. The water column had homogeneous properties at several stations occupied during TI08 (see Figure 2, e.g., stations 22 with ∼30.5 salinity, −5.5‰ $\delta^{18}O$, ∼−23% f_i and ∼33% f_r).

[16] The calculated fractions of river water and brine signal (neg. f_i) are relatively low in the bottom layer compared to maximum values. Stations with salinities above ∼30.5 occupied during TI08 show a well defined $\delta^{18}O$/salinity mixing line (Figure 7a). The intercept of the TI08 bottom layer $\delta^{18}O$/salinity correlation with the theoretical mixing line between river water and the Atlantic inflow end-members is at ∼33 salinity and −1‰ in $\delta^{18}O$ (Figure 7) and does not directly include the Atlantic inflow end-member values (34.92 salinity and 0.3‰ in $\delta^{18}O$).

Table 1. End-Member Values Used in Mass Balance Calculations[a]

End-Member	Salinity	$\delta^{18}O$ (‰)
Marine (f_{mar})	34.92(5)	0.3(1)
River (f_r)	0	−20(1)
Sea ice (f_i)	4(1)	surface +2.6(1) or −7+2.6(1)

[a]Numbers in parentheses are the estimated uncertainties within the last digit in our knowledge of each end-member value.

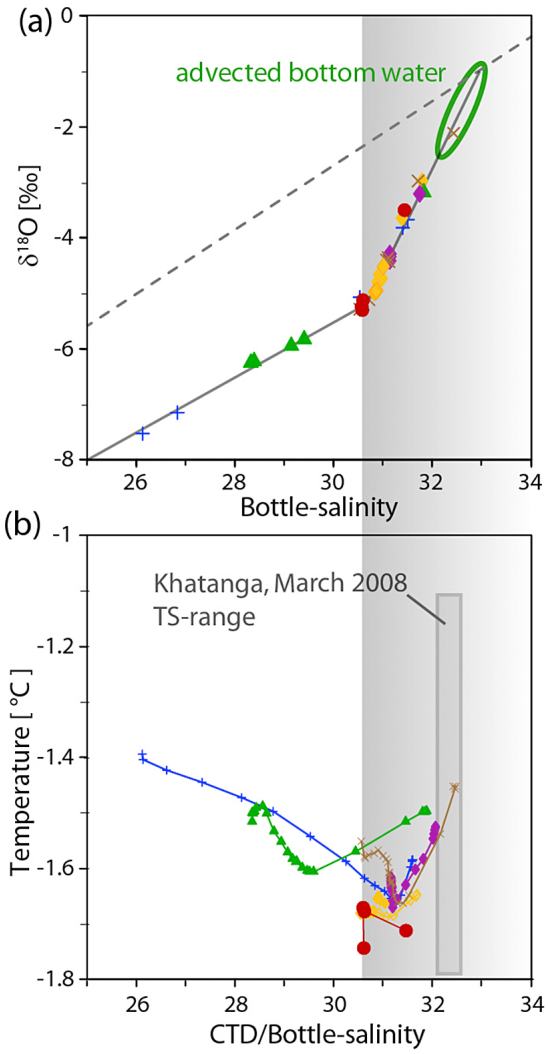

Figure 7. Stations with advected bottom water from TI08, i.e., stations with salinities above 30.5 (highlighted by gray shading). Figure 7a shows $\delta^{18}O$ versus bottle-salinity together with $\delta^{18}O$/salinity correlations (gray lines) and mixing line between river and Atlantic end-member (gray stippled). The signature of the advected bottom water is highlighted. Figure 7b shows temperature versus CTD-salinity (1 m averages) or bottle salinity for station 5 (dots) since no conductivity data are available for this station. Also indicated is the temperature/salinity range measured at mooring Khatanga (74°42.9′N, 125°17.4′E) during March 2008 [*Hölemann et al.*, 2011]. Station positions are shown within Figure 2 with corresponding symbols.

4.3. Sea Ice Formation During TI08

[17] A homogenous water column with high brine signal (neg. f_i) was observed at several positions across the study area (Figure 2, e.g., station 4 in the top row and station 22 in the bottom row) between 14 and 21 April 2008.

[18] There are spatial and temporal differences between stations, but the effect of the polynya on the water column is clearly marked by elevated brine signal in the surface layer or by uniform properties throughout the water column (Figure 2). Repeated sampling at our northernmost position (see red dots in Figure 2 at 131.25°E, 74.67°N for stations 5, 13, and 22 in top, middle, and bottom rows, respectively) documents the temporal development and shows that an enhanced brine signal in the polynya progresses from the surface layer into the bottom layer: On 14 April (Figure 2, sta. 5 in the top row) surface salinity was ~30.6 and fractions of brine signal (neg. f_i) and river water were ~20% and ~31%, respectively, in the surface layer, i.e., significantly higher than in the bottom layer (below 10 m) with ~12% and 20%, respectively and a salinity of 31.4. One week later on 21 April (Figure 2, sta. 13 in middle row) the gradient between surface and bottom layer was slightly smaller, but properties of the surface layer were unchanged and only the thickness of the surface layer had increased. Another week later on 29 April (Figure 2, sta. 22 in bottom row) the water column was completely mixed and had a salinity of ~30.5, but $\delta^{18}O$ values were slightly, but significantly, lower compared to before. Fractions of brine signal (neg. f_i) and river water thereby changed to ~23% and ~33%, respectively. While salinity in the surface layer remained constant at ~30.6 to 30.5, bottom salinities decreased from ~31.4 to 31.0, and finally to ~30.5 between 14 and 29 April.

4.4. Sea Ice Formation During TI09

[19] During our field campaign from 24 March to 23 April 2009 we observed elevated brine signals with similar values (neg. f_i) at intermediate depth (10 to 15 m) at all stations. At three northern stations the brine signal (neg. f_i) was highest in the surface layer (Figure 3 stations are marked in purple) and elevated values reached down to intermediate depth. At all stations the brine signal (neg. f_i) in the bottom layer remained relatively small compared to surface and intermediate layers. This indicates that polynya activity only altered the water column down to intermediate depth. For two shallow stations in the southeast of the study region (Figure 3, marked in green) the maximum brine signal (neg. f_i) extended to the bottom. These ~22 m deep stations were relatively shallow and separated from deeper waters in the northwest by a sill. Apparently previous convection due to sea ice formation in the polynya reached the bottom at this location and water masses containing the elevated brine signal (neg f_i) were retained by topographic barriers.

[20] Repeated sampling shows the evolution in the properties of the water column (see Figure 4, stations 8, 10, 13, 15 all at 128.58°E, 74.06°N). Between 8 and 23 April salinity and brine signal increased in the surface layer. Part of the salinity increase is additionally caused by a simultaneous decrease in river water fractions from nearly 80% to ~55% and increases of the Atlantic-derived fraction from 35% to 55% between 15 and 21 April (Figure 4, see sta. 10 and 13). Therefore, advection of waters with lower river water fractions must have occurred during this time period in addition to brine enrichment during sea ice formation.

4.5. Comparison of Inventories Between TI08 and TI09

[21] During TI09 average fractions of river water of ~41% were considerably higher than average river water fractions of ~30% observed during TI08. On the other hand, the average fraction of brine signal of ~15% (neg. f_i) during TI09 was lower compared to ~19% (neg. f_i) during TI08 (see Table 2). Inventory values can be derived by integrating the

Table 2. Average Inventories and Average Fractions ± Sigma for Stations Occupied During Programs TI08 and TI09[a]

		Sea Ice	River
TI08	inventory	−4.2 m ± 0.7 m	6.7 m ± 1.0 m
	fraction	−19% ± 3%	30% ± 4%
TI09	inventory	−3.7 m ± 0.7 m	10.1 m ± 1.5 m
	fraction	−15% ± 2%	41% ± 5%

[a]Average depth of water column was 22 m and 14 m for stations occupied during TI08 and TI09, respectively.

calculated fractions over depth. The river water inventories reflect the thickness of the water column consisting of pure river water and negative sea ice meltwater inventories reflect the thickness of water removed from the water column by sea ice formation. The derived average thickness of pure river water is 6.7 m and 10.1 m for TI08 and TI09, respectively. While the average thickness of water removed by sea ice formation is 4.2 m and 3.7 m for TI08 and TI09, respectively (see Table 2). The error for each inventory based on analytical errors alone is less than ± 0.1 m. While the difference in average river water inventories is large, the difference in average sea ice inventories is only 12% and within the standard deviation of each winter's station inventories.

5. Discussion

[22] Polynyas open during offshore winds and result in strongly enhanced sea ice production rates within the open water and thin-ice regions. This polynya activity is directly reflected in elevated brine signals (negative sea ice meltwater fractions f_i) derived from the δ^{18}O/salinity balance within the water column. As the brine signal in the water column is generally higher in winter than in summer data [*Bauch et al.*, 2009a, 2010] enhanced brine signals are assumed to result from the current winter's sea ice formation within the local polynyas.

[23] Although brines are released during sea ice formation, the brine signal (neg. f_i) is generally not increasing with depth. Instead the brine signal is generally highest in the surface layer and with further sea ice formation in the polynya the brine signal in the bottom layer gradually increases over time until the bottom layer shows the same value as the surface layer. While polynya-derived waters with elevated brine signals penetrated into the bottom layer during TI08, they only reached to intermediate depth during TI09. But average inventories of sea ice meltwater were similar at −4.2 m and −3.7 m during TI08 and TI09, respectively (compare also Table 2). Although the difference of 12% is significant, it seems relatively small to solely account for the observed differences in the vertical structure of the water column. It is the aim of the following discussion to further understand the processes which determine the impact of the coastal polynya on the water column. Since stratification and preconditioning is clearly important, we will compare salinity and δ^{18}O /salinity correlations from winter expeditions TI08 and TI09 with conditions in summers 2007 and 2008, respectively (section 5.1). The δ^{18}O/salinity signature also allows us to constrain the source of advected bottom water observed during TI08 (5.2). But which factors lead to the two layer structure seen in the δ^{18}O/salinity correlation? Is it mainly the influence of sea ice formation that determines the structure of the water column or is advection the dominant factor? To approach this question we will discuss the processes occurring in the Laptev Sea coastal polynya and their expected impact on the water column (5.3). Also we will constrain the factors determining the two smooth linear mixing lines in the salinity and δ^{18}O correlation (5.4).

5.1. Stratification and Preconditioning in Summers 2007 and 2008

[24] The surface hydrography of the Laptev Sea is strongly influenced by surface wind stress during summer [*Shpaikher et al.*, 1972; *Dmitrenko et al.*, 2005b; *Bauch et al.*, 2011b]. During this season freshwater discharge is maximum and the prevailing winds determine the fate of the Lena River plume. The river plume spreads predominantly northward under northwesterly winds, while southeasterly winds retain the Lena River plume in the southern Laptev Sea and the East Siberian Sea [*Guay et al.*, 2001; *Dmitrenko et al.*, 2005b, 2008b; *Bauch et al.*, 2011b]. These different modes for the spreading of the Lena River summer plume are also reflected in surface salinities in September 2007 and September 2008 (Figure 5). In summer 2007, alongshore winds advected the freshwater plume to the southeastern Laptev Sea and eastward, so that the surface layer to the north of the Lena delta was relatively saline (Figure 5a). In contrast, offshore winds in summer 2008 led to the accumulation of Lena River discharge north of the delta, and surface salinities there remained comparatively low (Figure 5b). The opposite preconditioning during the previous summers is directly reflected in different salinity and δ^{18}O ranges of surface water in our study area in April 2008 and April 2009 (Figure 6), while the bottom layer is largely unaffected. As a result the vertical salinity stratification observed during the 2008 field campaign was relatively weak (TI08, April–May) and strong during 2009 (TI09, March–April). According to different wind patterns during preceding summers, the average river water inventories of 6.7 m for TI08 and 10.1 m for TI09 (Table 2) show considerable differences as well. This is in agreement with a preservation of summer patterns throughout the entire winter season [*Dmitrenko et al.* 2010a; *Bauch et al.*, 2009b].

[25] Similar to salinity, δ^{18}O ranges are also different for TI08 and TI09, but there are also remarkable differences in the δ^{18}O/salinity relationship (see Figure 6). TI08 shows a pronounced offset of ∼2‰ in δ^{18}O at maximum brine fractions relative to the preceding summer 2007 δ^{18}O/salinity relationship at ∼30.5 salinity and ∼−5.5‰ in δ^{18}O (Figure 6a). While TI09 δ^{18}O data show no offset at this salinity, there is a smaller offset of ∼1‰ at maximum brine fractions relative to δ^{18}O/salinity relationship of the preceding summer 2008 at salinities of ∼23–27 and δ^{18}O of ∼−9–−7‰ (Figure 6b). Sea ice inventory values indicate that the amount of sea ice formed in each winter is similar. Therefore these differences in offsets within the δ^{18}O/salinity relationship are likely caused by different vertical distributions of the brine signal (neg. f_i) in the water column. This implies that depending on stratification polynyas can have different impacts on the water column of the Laptev Sea shelf.

5.2. Source of Bottom Water Advection in the Laptev Sea Coastal Polynya

[26] We observe separate, well defined mixing lines in the δ^{18}O/salinity relationship in 2008 (Figure 6a). The waters from the surface and inner shelf regime below a salinity of ~30.5 fall on a mixing line between river water and locally polynya-formed brine-enriched bottom water (Figure 2). Another mixing line is observed within the bottom layer above a salinity of ~30.5 between the polynya-formed bottom water at 30.5 and bottom waters with higher salinities (Figure 6 and Figure 7a). The intercept of the TI08 bottom layer δ^{18}O/salinity correlation with the theoretical direct mixing line between river water and the Atlantic inflow end-members is at ~33 salinity and −1‰ in δ^{18}O (Figure 7a) and thereby the linear δ^{18}O/salinity correlation in the bottom layer does not include the Atlantic inflow. This implies that the end-member of the saline bottom water found in the TI08 study area was already strongly modified relative to the Atlantic inflow. The calculated fractions of river water and brine signal are relatively low in the bottom layer and the waters are thereby clearly of non-local origin and can be assumed to be advected. This advected high salinity bottom water had a relatively cold temperature of −1.67°C at the beginning of our field campaign (see sta. 5 within Figure 7b). After a phase during which the polynya opened [see *Dmitrenko et al.*, 2010b; *Krumpen et al.*, 2011b] a saline but slightly warmer −1.45°C temperature bottom water was observed to replace the bottom layer in the entire study area (Figure 7b). Maximum salinities were ~31.4 before (Figure 2, see sta. 5 in top row and Figure 7b) and ~32.4 after the polynya opening (Figure 2, bottom row, and Figure 7b), although these differences may result from different station position and sampling depth (Figure 2). As all signatures of advected bottom water fall on a uniform mixing line between locally formed polynya water (~30.5 salinity) and a uniform high salinity end-member (Figure 7a) the origin of the advected bottom water cannot be isotopically distinguished. Instead the identical mixing line suggests a common source although salinity and temperatures are not identical.

[27] The general circulation of the upper waters is from west to east along the Eurasian continental slope [*Newton et al.*, 2008]. This agrees with estimates from dynamic ocean topography which suggest eastward transport of water on the inner Laptev Sea shelf with ~10 cm/s in April 2008 [*Kwok and Morison*, 2011]. Long-term current measurements from moored instruments on the Laptev Sea shelf (see location of mooring Khatanga in Figure 1) show that on average the annual water transport in the bottom layer is directed eastward [*Bauch et al.*, 2010]. This west to east transport of saline bottom water balances the northward export of fresh surface waters and brine-enriched bottom waters in the eastern Laptev Sea [*Bauch et al.*, 2009a]. Thus we assume that on average bottom waters from the northwestern Laptev Sea provide a permanent advective source to the inner Laptev Sea shelf. Near-bottom currents at mooring Khatanga during both winter expeditions TI08 and TI09 were predominantly oriented southward and their average velocities were 4.8 cm/s and 2.2 cm/s, respectively. The properties of the bottom water have to fall on the high salinity mixing line defined by the δ^{18}O/salinity above ~30.5 salinity observed during TI08 (Figure 7; compare also Figure 2c). Since waters with a net positive sea ice meltwater contribution are generally absent within the bottom layer [*Bauch et al.*, 2005, 2009a, 2010] the properties of the remote source of the bottom water have to be lower or equal to ~33 salinity and −1‰ in δ^{18}O, which is the intercept of the TI08 bottom layer δ^{18}O/salinity correlation within the theoretical mixing line between river water and the Atlantic layer end-member (Figure 7a). In summer 2007 bottom waters with a suitable salinity of 33.05 were observed in the northwestern Laptev Sea, but with a lower δ^{18}O of −1.6‰ (e.g., sta. IP007P at 123.01°E 75.34°N with a bottom water temperature of −1.67°C). Salinity values in the advected bottom water observed during TI08 match δ^{18}O/salinity signatures of bottom water observed in summer 2007 in the study region (Figure 6a). The difference in δ^{18}O may therefore be caused by inter annual variability of seasonal water mass modification in the region.

[28] Upper halocline waters with an Atlantic-derived temperature signal penetrate the outer Laptev Sea shelf and it has been speculated, that a slight temperature increase, along with a salinity increase might indicate an Atlantic-derived heat source even on the inner Laptev Sea shelf [*Dmitrenko et al.*, 2010b]. However, vertical transport of surface heat into the bottom layer by mixing of the water column has been observed over shallow banks in the western Laptev Sea [*Bauch et al.*, 2010] and year-round mooring data document high temperature excursions of up to 3°C coincident with episodes of lower bottom water salinity during autumn and winter [*Hölemann et al.*, 2011]. As temperature and salinity variations observed to the northwest of our study area at mooring Khatanga in March 2008 (Figure 7b) are considerably higher than differences in observed bottom water properties, a local heat source on the shelf seems likely. Identical δ^{18}O/salinity signatures (Figure 7a) indicate an identical modification history of bottom water signatures on the western shelf. Western or northwestern Laptev Sea bottom waters may therefore be the source of the advected bottom water observed before and after the TI08 polynya opening.

5.3. Mechanisms of Water Column Modification in the Coastal Polynya

[29] The most likely mechanisms that may be responsible for vertical changes in the water column are wind and possibly tide-induced turbulent vertical mixing [*Hölemann et al.*, 2011], brine-related convective overturning and variable advection patterns. The expected impact of each mechanism on the water column is compared with the observed changes in the Laptev Sea coastal polynya during winter.

[30] Turbulent vertical mixing throughout the water column will produce a uniform water body at the average properties of the original water column and as sea ice formation releases brines salinity will be proportionally higher (Figure 8a). Observations from TI08 show a decrease in bottom layer salinity during polynya activity and an increase in fractions of river water and brine signal (Figure 2, stations 5, 13, 22; compare description in section 4.3) as expected from turbulent mixing (Figure 8a). However, the surface layer remained at a constant salinity of ~30.5 and did not increase as would have been the case, if turbulent vertical mixing was the predominant factor for water column transformation in the Laptev Sea coastal polynya. In contrast to

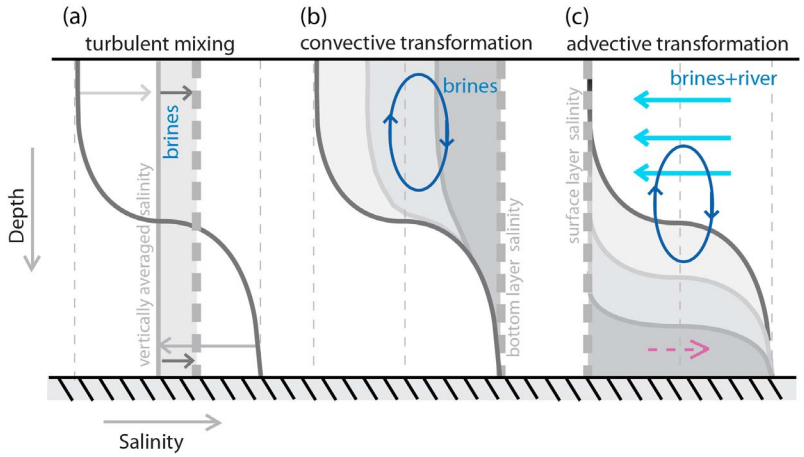

Figure 8. Schematic sketch of different mechanisms transforming a typical salinity profile (dark gray) to constant properties (thick stippled line) in the Laptev Sea coastal polynya. During turbulent mixing (Figure 8a) the entire water column is mixed to constant properties at the vertically averaged salinity (light gray arrows and light gray line) increased by brines (dark gray arrows). During convective transformation of the water column (Figure 8b) the addition of brines gradually increases salinity in the surface layer until bottom salinity is reached. During predominant advective transformation (Figure 8c) the saline bottom layer is gradually replaced by low salinity surface waters with high river water content and brine signal inserted by the polynya at a different position.

TI08, surface salinities increased concurrent with an increase in brine signal (neg. f_i) during TI09 (Figure 4, stations 8, 10, 13, 15; compare description in section 4.4). These changes suggest convective transformation by sea ice formation as bottom layer salinities remain constant (Figure 8b) in addition to advection of marine waters with lower fractions of river water (see section 4.4). The offshore winds necessary for an opening of the polynya favor transport of surface water from west to east. An eastward advection of surface waters would likely add surface water with reduced river water fractions which generally decrease with distance from the Lena River Delta as is also supported by our observations.

[31] During polynya activity in TI08 the surface layer remained at constant salinity with high fractions of river water and brine signal over time (Figure 2, stations 5, 13, 22 as described in section 4.3) and the properties of the bottom layer were clearly not altered by turbulent (Figure 8a) or convective mixing (Figure 8b). The surface layer with a constantly high brine signal could have been advected during the polynya opening and then gradually mixed downward into the intermediate and bottom layers by turbulent or convective overturning (Figure 8c). Increased near-surface advection during the polynya opening likely occurred when the near-bottom flow was reduced (see Figure 8c) relative to enhanced near bottom flow observed before and after the polynya openings during TI08 [*Dmitrenko et al.*, 2010b].

5.4. Mixing Processes Reflected in δ^{18}O/Salinity Relationship

[32] The δ^{18}O/salinity relationship shows two well defined mixing lines for our data set from late winter 2008 (TI08) when enhanced signals of sea ice formation reached the bottom layer. These correlations represent mixing lines and any water sample can be clearly described as variable mixture of pairs of three water types: river water, polynya-produced water and saline bottom water from the northwestern Laptev Sea. The inner shelf and surface layer is a mixture of river water and the polynya-produced water at ~30.5 salinity and δ^{18}O of −5.5‰ during TI08 (Figures 2 and 6). The bottom layer is a mixture of polynya-produced water and saline bottom water from the northwestern Laptev Sea (see section 5.2). This local polynya-produced water with maximum brine signals and similar salinity/δ^{18}O was also predominant in the eastern Laptev Sea bottom layer during the summers of 1994 [*Bauch et al.*, 2009a] and 2008 (Figure 6). In late winter 2009 (TI09) enhanced impact of sea ice formation reached only to intermediate depth. As a result the δ^{18}O/salinity correlation in winter 2009 does not show a uniform mixing scheme and the maximum brine signal (neg. f_i) is seen within the surface layer (Figure 3 and Figure 6). It may be speculated that the conditions seen in winter 2009 (TI09) are similar to those observed in summer 2007 when maximum brine signals were observed in the surface [*Bauch et al.*, 2010].

[33] The question remains which factors led to the two layer structure seen in the two linear mixing lines in the salinity and δ^{18}O correlation. Is it mainly the amount of newly formed sea ice that determines the structure of the water column or are preconditioning and advection of surface and bottom waters the predominant factors? The formation of brine-enriched bottom water in the polynyas is a necessary prerequisite and depends on the amount of sea ice derived brines in relation to the prevailing stratification. But the generation of two well defined mixing lines is likely the result of gradual vertical mixing possibly as a result of strong vertical shear [*Hölemann et al.*, 2011]. Maximum brine influence is seen in polynya-derived waters in the bottom layer during TI08 and at intermediate depth during TI09 (see Figure 6, dots with blue/purple coloring). This shift of sea ice derived brines within the water column is reflected in different patterns in f_i/f_r ratios between TI08 and TI09 (Figure 9). The ratios of f_i/f_r are nearly constant within the

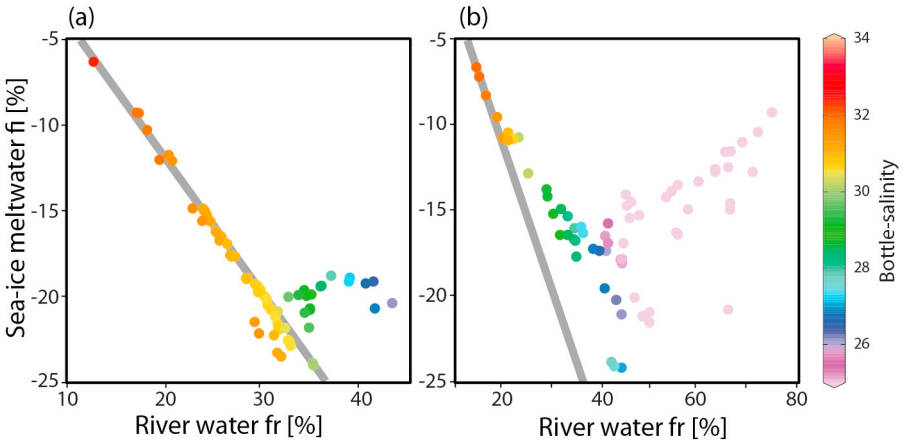

Figure 9. Relative contributions of sea ice meltwater fraction f_i versus river water fraction f_r for all station data obtained during (a) TI08 and (b) TI09. The coloring of each dot indicates the salinity. The bottom layer observed during TI08 has a constant ratio f_i/f_r and is highlighted by a gray line. The same line is shown for comparison together with station data obtained during TI09. Please note common scale for f_i and different scales for f_r in Figures 9a and 9b.

bottom layer during TI08 and the constant ratios reflect the gradual mixing between local polynya-formed water and advected bottom water from the western Laptev Sea with a wide range of f_i and f_r values (Figure 9a). During TI09 the ratios of f_i/f_r are also constant within the bottom layer, although local polynya water with relatively high absolute f_i and f_r values is absent. Accordingly the f_i and f_r range with constant f_i/f_r ratios is small and reflects the advected bottom water from the western Laptev Sea only. The change in f_i/f_r ratios within the intermediate layer (see salinity range of ~26–31 within Figure 9b) suggests that vertical turbulent mixing in TI09 is not strong enough to create a uniform mixing line across the remaining stratification. During TI08, on the other hand, stratification was weak enough so that advection and possibly shear-induced vertical mixing resulted in smooth and uniform mixing lines.

6. Summary and Conclusions

[34] Hydrographic and stable oxygen isotope observations in the Laptev Sea coastal polynyas document the signature of sea ice formation and show that the water column is significantly affected by preconditioning of freshwater from the preceding summer, as well as by advection of bottom waters.

[35] The effects of sea ice formation are directly observed in the δ^{18}O/salinity signature. The signal of brines released during sea ice formation is generally decreasing with depth during winter and shows reduced values in the bottom layer. When sea ice formation affects the entire water column the bottom layer signal increases and approaches the surface layer values. A local brine-enriched bottom water type with relatively high river water fractions was formed in the southeastern Laptev Sea coastal polynya at a salinity of ~30.5 and δ^{18}O of ~−5.5‰ during winter 2007/2008. The polynya-formed local bottom water has the lowest salinities observed within the bottom layer. In general, the δ^{18}O/salinity correlation shows two well defined linear mixing lines. Surface layer or inner shelf waters are a mixture of river water and the polynya-formed brine-enriched bottom water. On the other hand, the bottom layer is characterized by a mixture of polynya-formed brine-enriched bottom water and relatively high salinity bottom water advected from the western or northwestern Laptev Sea. Gradual turbulent mixing within the bottom layer likely smoothes the δ^{18}O/salinity mixing line.

[36] Although winds are essential in forcing a polynya opening, wind-induced turbulent mixing is not the primary mechanism reflected in the transformation of the water column. Instead it appears that convective overturning combined with near-bottom flow transformed the water column in both years. Advection of saline bottom water following polynya openings [*Dmitrenko et al.*, 2010b] showed salinity and temperature variations well within the range of variability seen in year-round bottom moorings [*Hölemann et al.*, 2011]. The homogeneous δ^{18}O/salinity signature of the advected bottom water indicates a common source with a similar modification history, likely on the western or northwestern Laptev Sea shelf.

[37] Inventories of sea ice meltwater fractions of −4.2 and −3.7 m were comparable between both years. Although polynya activity is reflected in the amount of sea ice produced, its influence on the structure of the water column does not primarily depend on the amount of sea ice formed, but on the (freshwater) preconditioning from the preceding summer. Summer preconditioning is controlled by summer wind patterns that may be regional and not captured by arctic-wide indices [*Bauch et al.*, 2011b]. However, the observed advection of bottom waters also significantly determines the structure of the water column and further investigations are necessary to determine if advection patterns are directly related to the wind-forcing necessary to open polynyas or to the relatively fresh water transported into the bottom layer by the polynyas.

[38] Polynya activity determines the general structure of the water column although the estimated amount of sea ice formed in coastal polynyas relative to the total amount is only ~10% in the Laptev Sea [*Willmes et al.*, 2011]. Our study indicates that changes in summer wind conditions have a

considerable impact on Laptev Sea bottom water that is exported northward in the eastern Laptev Sea [*Bauch et al.*, 2009a]. Prolonged ice free periods will potentially increase the impact of summer atmospheric forcing on the shelf and as a consequence on shelf-derived Arctic Ocean halocline waters. Our results indicate that shelf processes and the feedback between sea ice processes and the ongoing climate change are not likely to be predictable in general assessments. Further field studies are necessary to bridge the gap between shelf processes and large-scale impacts. Future observations will have to show how variable these processes are and whether they are permanently altered by long-term changes.

[39] **Acknowledgments.** We are grateful to all of our Russian and German colleagues who made it possible to successfully conduct our field-work program in the Laptev Sea coastal polynya region in late winters 2008 and 2009. This work was part of the German-Russian cooperation "System Laptev Sea" funded by the BMBF under grant 03G0639D as well as by Roshydromet and the Russian Ministry of Education and Science. We thank R. Newton and P. Schlosser for helpful comments.

References

Aagaard, K., L. Coachman, and E. Carmack (1981), On the halocline of the Arctic Ocean, *Deep Sea Res.*, *28*, 529–545, doi:10.1016/0198-0149(81)90115-1.

Aagaard, K., J. H. Swift, and E. C. Carmack (1985), Thermohaline circulation in the Arctic Mediterranean Sea, *J. Geophys. Res.*, *90*(C3), 4833–4846, doi:10.1029/JC090iC03p04833.

Bareiss, J., and K. Görgen (2005), Spatial and temporal variability of sea ice in the Laptev Sea: Analyses and review of satellite passive-microwave data and model results, 1979 to 2002, *Global Planet. Change*, *48*, 28–54, doi:10.1016/j.gloplacha.2004.12.004.

Bauch, D., P. Schlosser, and R. F. Fairbanks (1995), Freshwater balance and the sources of deep and bottom waters in the Arctic Ocean inferred from the distribution of $H_2^{18}O$, *Prog. Oceanogr.*, *35*, 53–80, doi:10.1016/0079-6611(95)00005-2.

Bauch, D., H. Erlenkeuser, and N. Andersen (2005), Water mass processes on Arctic shelves as revealed from ^{18}O of H_2O, *Global Planet. Change*, *48*, 165–174, doi:10.1016/j.gloplacha.2004.1012.1011.

Bauch, D., I. A. Dmitrenko, C. Wegner, J. Hölemann, S. A. Kirillov, L. A. Timokhov, and H. Kassens (2009a), Exchange of Laptev Sea and Arctic Ocean halocline waters in response to atmospheric forcing, *J. Geophys. Res.*, *114*, C05008, doi:10.1029/2008JC005062.

Bauch, D., I. A. Dmitrenko, S. A. Kirillov, C. Wegner, J. Hölemann, S. Pivovarov, L. A. Timokhov, and H. Kassens (2009b), Eurasian Arctic shelf hydrography: Exchange and residence time of southern Laptev Sea waters, *Cont. Shelf Res.*, *29*, 1815–1820, doi:1810.1016/j.csr.2009.1806.1009.

Bauch, D., J. Hölemann, S. Willmes, M. Gröger, A. Novikhin, A. Nikulina, H. Kassens, and L. Timokhov (2010), Changes in distribution of brine waters on the Laptev Sea shelf in 2007, *J. Geophys. Res.*, *115*, C11008, doi:10.1029/2010JC006249.

Bauch, D., M. Rutgers van der Loeff, N. Andersen, S. Torres-Valdes, K. Bakker, and E. P. Abrahamsen (2011a), Origin of freshwater and polynya water in the Arctic Ocean halocline in summer 2007, *Prog. Oceanogr.*, *91*, 482–495, doi:10.1016/j.pocean.2011.07.017

Bauch, D., M. Gröger, I. Dmitrenko, J. Hölemann, S. Kirillov, A. Mackensen, E. Taldenkova, and N. Andersen (2011b), Atmospheric controlled freshwater water release at the Laptev Sea continental margin, *Polar Res.*, *30*, 5858, doi:10.3402/polar.v30i0.5858.

Coachman, L. K., and C. A. Barnes (1963), The movement of Atlantic Water in the Arctic Ocean, *Arctic*, *16*(1), 8–16.

Comiso, J. C., C. L. Parkinson, R. Gersten, and L. Stock (2008), Accelerated decline in the Arctic sea ice cover, *Geophys. Res. Lett.*, *35*, L01703, doi:10.1029/2007GL031972.

Cooper, L. W., J. W. McClelland, R. M. Holmes, P. A. Raymond, J. J. Gibson, C. K. Guay, and B. J. Peterson (2008), Flow-weighted values of runoff tracers ($\delta^{18}O$, DOC, Ba, alkalinity) from the six largest Arctic rivers, *Geophys. Res. Lett.*, *35*, L18606, doi:10.1029/2008GL035007.

Craig, H. (1961), Standard for reporting concentrations of deuterium and oxygen-18 in natural waters, *Science*, *133*, 1833–1834, doi:10.1126/science.133.3467.1833.

Dmitrenko, I. A., K. N. Tyshko, S. A. Kirillov, H. Eicken, J. A. Hölemann, and H. Kassens (2005a), Impact of flaw polynyas on the hydrography of the Laptev Sea, *Global Planet. Change*, *48*, 9–27, doi:10.1016/j.gloplacha.2004.12.016.

Dmitrenko, I. A., S. A. Kirillov, H. Eicken, and N. Markova (2005b), Wind-driven summer surface hydrography of the eastern Siberian shelf, *Geophys. Res. Lett.*, *32*, L14613, doi:10.1029/2005GL023022.

Dmitrenko, I. A., I. V. Polyakov, S. A. Kirillov, L. A. Timokhov, I. E. Frolov, V. T. Sokolov, H. L. Simmons, V. V. Ivanov, and D. Walsh (2008a), Toward a warmer Arctic Ocean: Spreading of the early 21st century Atlantic Water warm anomaly along the Eurasian Basin margins, *J. Geophys. Res.*, *113*, C05023, doi:10.1029/2007JC004158.

Dmitrenko, I. A., S. A. Kirillov, and L. B. Tremblay (2008b), The long-term and interannual variability of summer fresh water storage over the eastern Siberian shelf: Implication for climatic change, *J. Geophys. Res.*, *113*, C03007, doi:10.1029/2007JC004304.

Dmitrenko, I. A., S. A. Kirillov, T. Krumpen, M. Makhotin, E. P. Abrahamsen, S. Willmes, E. Bloshkina, J. A. Hölemann, H. Kassens, and C. Wegner (2010a), Wind-driven diversion of summer river runoff preconditions the Laptev Sea coastal polynya hydrography: Evidence from summer-to-winter hydrographic records of 2007–2009, *Cont. Shelf Res.*, *30*, 1656–1664, doi:10.1016/j.csr.2010.06.012.

Dmitrenko, I. A., S. A. Kirillov, L. B. Tremblay, D. Bauch, J. A. Hölemann, T. Krumpen, H. Kassens, C. Wegner, G. Heinemann, and D. Schröder (2010b), Impact of the Arctic Ocean Atlantic water layer on Siberian shelf hydrography, *J. Geophys. Res.*, *115*, C08010, doi:10.1029/2009JC006020.

Frank, M. (1996), Spurenstoffuntersuchungen zur Zirkulation im Eurasischen Becken des Nordpolarmeeres, Ph.D. thesis, 100 pp., Univ. of Heidelberg, Heidelberg, Germany.

Guay, C. K., K. K. Falkner, R. D. Muench, M. Mensch, M. Frank, and R. Bayer (2001), Wind-driven transport pathways for Eurasian Arctic river discharge, *J. Geophys. Res.*, *106*(C6), 11,469–411,480.

Hölemann, J. A., S. Kirillov, T. Klagge, A. Novikhin, H. Kassens, and L. Timokhov (2011), Observations of near-bottom water warming in the Laptev Sea in response to increased summertime surface water temperatures, *Polar Res.*, *30*, 6425, doi:10.3402/polar.v6430i6420.6425.

Krumpen, T., S. Willmes, M. A. Morales Maqueda, C. Haas, J. A. Hölemann, R. Gerdes, and D. Schröder (2011a), Evaluation of a polynya flux model by means of thermal infrared satellite estimates, *Ann. Glaciol.*, *52*(57), 52–60, doi:10.3189/172756411795931615.

Krumpen, T., et al. (2011b), Sea ice production and water mass modification in the eastern Laptev Sea, *J. Geophys. Res.*, *116*, C05014, doi:10.1029/2010JC006545.

Kwok, R., and J. Morison (2011), Dynamic topography of the ice covered Arctic Ocean from ICESat, *Geophys. Res. Lett.*, *38*, L02501, doi:10.1029/2010GL046063.

Kwok, R., and D. A. Rothrock (2009), Decline in Arctic sea ice thickness from submarine and ICESat records: 1958–2008, *Geophys. Res. Lett.*, *36*, L15501, doi:10.1029/2009GL039035.

Kwok, R., G. F. Cunningham, M. Wensnahan, I. Rigor, H. J. Zwally, and D. Yi (2009), Thinning and volume loss of the Arctic Ocean sea ice cover: 2003–2008, *J. Geophys. Res.*, *114*, C07005, doi:10.1029/2009JC005312.

Létolle, R., J. Martin, A. Thomas, V. Gordeev, S. Gusarova, and I. Sidorov (1993), ^{18}O abundance and dissolved silicate in the Lena delta and Laptev Sea (Russia), *Mar. Chem.*, *43*, 47–64, doi:10.1016/0304-4203(93)90215-A.

Melling, H., and R. Moore (1995), Modification of halocline source waters during freezing on the Beaufort Sea shelf: Evidence from oxygen isotopes and dissolved nutrients, *Cont. Shelf Res.*, *15*, 89–113, doi:10.1016/0278-4343(94)P1814-R.

Newton, R., P. Schlosser, D. G. Martinson, and W. Maslowski (2008), Freshwater distribution in the Arctic Ocean: Simulation with a high resolution model and model-data comparison, *J. Geophys. Res.*, *113*, C05024, doi:10.1029/2007JC004111.

Östlund, H., and G. Hut (1984), Arctic Ocean water mass balance from isotope data, *J. Geophys. Res.*, *89*(C4), 6373–6381, doi:10.1029/JC089iC04p06373.

Pfirman, S., W. Haxby, H. Eicken, M. Jeffries, and D. Bauch (2004), Drifting Arctic sea ice archives changes in ocean surface conditions, *Geophys. Res. Lett.*, *31*, L19401, doi:10.1029/2004GL020666.

Polyakov, I., et al. (2007), Observational program tracks Arctic Ocean transition to a warmer state, *Eos Trans. AGU*, *88*(40), 398, doi:10.1029/2007EO400002.

Schauer, U., E. Fahrbach, S. Osterhus, and G. Rohardt (2004), Arctic warming through the Fram Strait: Oceanic heat transport from 3 years of measurements, *J. Geophys. Res.*, *109*, C06026, doi:10.1029/2003JC001823.

Schlosser, P., D. Bauch, G. Bönisch, and R. F. Fairbanks (1994), Arctic river-runoff: Mean residence time on the shelves and in the halocline, *Deep Sea Res., Part I*, *41*(7), 1053–1068, doi:10.1016/0967-0637(94)90018-3.

Shpaikher, O., Z. P. Federova, and Z. S. Yankina (1972), Interannual variability of hydrological regime of the Siberian shelf seas in response to atmospheric processes (in Russian), *Proc. Arct. Antarct. Res. Inst.*, *306*, 5–17.

Steele, M., and T. Boyd (1998), Retreat of the cold halocline layer in the Arctic Ocean, *J. Geophys. Res.*, *103*(C5), 10,419–410,435.

Willmes, S., S. Adams, D. Schroeder, and G. Heinemann (2011), Spatio-temporal variability of sea ice coverage, polynya dynamics and ice production in the Laptev Sea between 1979 and 2008, *Polar Res.*, *30*, 5971, doi:10.3402/polar.v30i0.5971.

Zakharov, V. F. (1966), The role of flaw leads off the edge of fast ice in the hydrological and ice regime of the Laptev Sea, *Oceanology, Engl. Transl.*, *6*(1), 815–821.

Zakharov, V. F. (1997), Sea ice in the climate system, *Rep. WMO/TD 782*, 80 pp., World Clim. Res. Programme, World Meteorol. Organ., Geneva, Switzerland.

D. Bauch, I. A. Dmitrenko, and H. Kassens, GEOMAR Helmholtz Centre for Ocean Research Kiel, Wischhofstr. 1-3, D-24148 Kiel, Germany.

J. A. Hölemann, M. A. Janout, and T. Krumpen, Alfred Wegener Institute for Polar and Marine Research, Am Handelshafen 12, D-27570 Bremerhaven, Germany.

S. A. Kirillov and L. Timokhov, Arctic and Antarctic Research Institute, 38 Bering Str., St. Petersburg, Russia, 199397.

A. Nikulina, Academy Mainz, c/o GEOMAR, Wischhofstr. 1-3, D-24148 Kiel, Germany.